NAR Cancer, 2025, **7**, zcaf018
https://doi.org/10.1093/narcan/zcaf018
Cancer Gene Regulation, Chromatin, and Epigenetics

GSK-3484862, a DNMT1 degrader, promotes *DNMT3B* expression in lung cancer cells

Qin Chen[1], Swanand Hardikar[1], Kimie Kondo[1], Nan Dai[2], Ivan R. Corrêa Jr[2], Meigen Yu[1], Marcos R. Estecio[1], Xing Zhang[1], Taiping Chen[1,*], Xiaodong Cheng[1,*]

[1]Department of Epigenetics and Molecular Carcinogenesis, University of Texas MD Anderson Cancer Center, Houston, TX 77030, United States
[2]New England Biolabs, Inc., Ipswich, MA 01938, United States

[*]To whom correspondence should be addressed. Email: tchen2@mdanderson.org
Correspondence may also be addressed to Xiaodong Cheng. Email: xcheng5@mdanderson.org

Abstract

DNA methylation alterations, including hypermethylation and silencing of tumor suppressor genes, contribute to cancer formation and progression. The FDA-approved nucleoside analogs azacytidine and decitabine are effective demethylating agents for hematologic malignancies but their general use has been limited by their toxicity and ineffectiveness against solid tumors. GSK-3484862, a dicyanopyridine-containing, DNMT1-selective inhibitor and degrader, offers a promising lead for developing novel demethylating therapeutics. Here, we demonstrate that GSK-3484862 treatment upregulates *DNMT3B* expression in lung cancer cell lines (A549 and NCI-H1299). Disrupting *DNMT3B* in NCI-H1299 sensitizes these cells to GSK-3484862, enhancing its inhibitory effects on cell viability and growth. GSK-3484862 treatment induces demethylation at *DNMT3B* regulatory elements including a candidate enhancer located ~10 kb upstream of the *DNMT3B* transcription start site, as well as at the promoter of *TERT* (telomerase reverse transcriptase), a potential activator of *DNMT3B* expression. These demethylation events correlate with upregulation of *DNMT3B* expression. These findings suggest that combining inhibitors targeting DNMT1, the maintenance methyltransferase, with those targeting DNMT3A/3B, the *de novo* methyltransferases, or using pan-DNMT inhibitors, could enhance anticancer efficacy and reduce resistance.

Graphical abstract

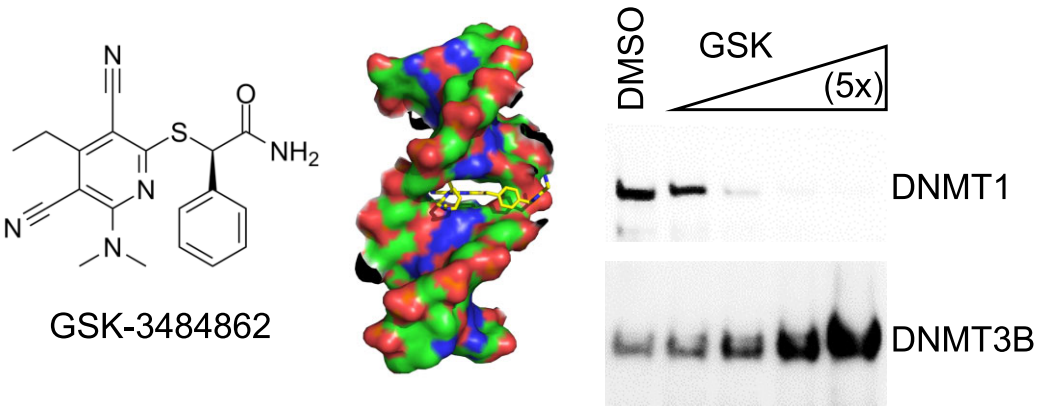

Introduction

DNA methylation, particularly at CpG dinucleotides within promoters, is a key epigenetic modification that can silence gene expression [1]. Early studies demonstrated the role of promoter CpG hypermethylation in transcriptional repression, including the silencing of β-globin genes [2–4] and tumor-suppressor genes, such as retinoblastoma (*RB*) [5, 6], von Hippel–Lindau (*VHL*) [7–9], *p16/CDKN2* [10–12], and RAS association domain family 1A (*RASSF1A*) [13–16]. Although the mechanisms underlying aberrant DNA hypermethylation in tumor suppressor genes are complex and not fully understood, DNA hypomethylating agents are actively used as cancer therapies, either as stand-alone treatments or in combination with other approaches.

The FDA-approved DNA hypomethylating agents decitabine (5-aza-2′-deoxycytodine) and azacitidine

Received: January 22, 2025. **Editorial Decision:** May 13, 2025. **Accepted:** May 15, 2025

(Vidaza) are cytidine analog prodrugs that, after metabolic conversion to their triphosphate form, are incorporated into DNA or RNA during replication or transcription [17–20]. These agents have been used in clinical settings, particularly for treating hematological disorders such as myelodysplastic syndromes and acute myeloid leukemia (AML), especially in older or medically fragile patients [21]. However, these drugs face significant limitations, including dose-limiting toxicity, poor tolerance in patients, limited median overall survival for elderly patients, and ineffectiveness against solid tumors [22–25].

These challenges have spurred efforts to develop non-nucleoside DNA methyltransferase (DNMT) inhibitors, particularly targeting the maintenance enzyme DNMT1 [26, 27]. One promising advancement toward these inhibitors is the development of a class of non-nucleoside, dicyanopydridine-containing DNMT1-selective inhibitors by GlaxoSmithKline (GSK) [28, 29]. Among these, GSK-3484862, the purified *R*-enantiomer of GSK-3482364, has been studied *in vitro*, in cells, and in animals. In a transgenic mouse model of sickle cell disease, oral administration of GSK-3482364 was well tolerated and significantly increased both fetal hemoglobin levels and the percentage of erythrocytes expressing fetal hemoglobin [30]. In murine embryonic stem cells (mESCs), GSK-3484862 treatment achieved DNA hypomethylation levels similar to those observed in *Dnmt1* knockout (KO) mESCs [31].

GSK-3484862 works by targeting DNMT1 for protein degradation in mESCs and various cancer cell lines [32]. In AML cell lines (THP1 and OCI-AML3), GSK-3484862 modulated the expression level of *FOXN3-AS1*, a long noncoding RNA transcribed from the antisense strand of the *FOXN3* gene [33]. Additionally, delivery of GSK-3484862 into tumor cells triggered tumor cell pyroptosis, a form of programmed cell death, in the 4T1 breast tumor mouse model [34]. Furthermore, GSK-3484862 treatment upregulated odontoblast-related genes in primary dental mesenchymal cells isolated from E14.5 mouse tooth germs [35].

Treatment of MV4-11 leukemia cells with GSK-3685032 (a chemical analog to GSK-3484862) showed a relatively slow onset of growth inhibition (≥3 days), with increasing potency over a 6-day period [28]. In a mouse model of AML, GSK-3685032 demonstrated superior tumor regression compared to decitabine [28]. However, repeated treatment with escalating doses of GSK-3685032 (50 nM to >30 μM) over several months in colorectal cancer cell lines (HCT116 and RKO) led to resistance and retention of DNA methylation on the X-chromosome [36]. This retention of chromosome-specific methylation was associated with increased expression of *DNMT3A2* [36]—an isoform of the *de novo* DNA methyltransferase DNMT3A [37]. In this study, we report that treatment of lung cancer cell lines (A539 and NCI-H1299) with doses of GSK-3484862 in 0.1–4 μM significantly increased the expression of *DNMT3B* concurrent with rapid depletion of DNMT1 protein. DNA methylation analysis suggests that GSK-3484862-induced hypomethylation of predicted regulatory elements in the *DNMT3B* gene contributes to its upregulation. Furthermore, deletion of *DNMT3B* in NCI-H1299 cells, by CRISPR/Cas9 gene editing, inhibited cell growth and sensitized these cells to GSK-3484862 treatment, highlighting the potential therapeutic interplay between DNMT3B and DNMT1.

Materials and methods

Chemicals

GSK-3484862 (Cat. #HY-135146) and GSK-3685032 (Cat. #HY-139664) were purchased from MedChemExpress. Compounds were dissolved in 100% dimethyl sulfoxide (DMSO), aliquoted, and stored at −80°C prior to use.

Antibodies

The following primary antibodies were used in this study: DNMT1 [Cell Signaling Technology (CST), Cat. #5032], DNMT3A (CST, Cat. #3598), DNMT3B (CST, Cat. #72335), H3 (CST, Cat. #14269), GAPDH (CST, Cat. #2118), actin (Sigma, Cat. #A2228), and vinculin (Sigma, Cat. #SAB4200729). The secondary antibodies used in this study were horseradish peroxidase (HRP)-linked anti-rabbit-IgG (CST, Cat. #7074) and HRP-linked anti-mouse-IgG (Abcam, Cat. #ab6820). Two DNMT3B monoclonal antibodies (#72335 and #67259) were developed by CST (Supplementary Fig. S1A and B). However, antibody #67259 showed a nonspecific binding between 60 and 75 kDa (Supplementary Fig. S1C–F). Therefore, we exclusively used #72335 in this study.

Cell lines and culture

Non-small cell lung cancer cell lines A549 and NCI-H1299 were purchased from the American Type Culture Collection (ATCC) and validated at the University of Texas MD Anderson Cancer Center (Houston, TX). A549 cells were cultured in ATCC-formulated F-12K medium (Cat. #30-2004) supplemented with 10% fetal bovine serum (FBS, Sigma) and 1% penicillin/streptomycin. NCI-H1299 cells were cultured in RPMI1640 medium supplemented with 10% FBS, 1% penicillin/streptomycin, 2 mM L-glutamine (Mediatech), and 10 mM HEPES (Mediatech). Cells were incubated at 37°C with 5% CO_2.

Chemical compound treatment

Cells were seeded onto 6- or 12-well culture plates at a density of 1–3 × 10^5 cells per well. The following day, the culture medium was replaced with fresh culture medium containing either 0.1% DMSO or GSK compounds at the concentrations (from 0.1 to 4 μM) specified in the figures. The medium, supplemented with either 0.1% DMSO or fresh compound, was refreshed every other day. At the time points (from 0.5 to 10 days) designated in the figures, cells were harvested for western blot analysis, reverse transcriptase quantitative polymerase chain reaction (RT-qPCR), and genomic DNA methylation assays, as described previously [32].

Western blot

Cells were seeded into each well of culture plates at approximately equal densities. After overnight incubation, the cells were treated with either 0.1% DMSO or the GSK compound at the specified doses. At the indicated time points, DMSO- or compound-treated cells were lysed using sodium dodecyl sulfate (SDS) sample buffer. The whole cell lysates were then separated by Bis-Tris sodium dodecyl sulfate–polyacrylamide gel electrophoresis (SDS–PAGE) using precast 4%–20% polyacrylamide gels (Bio-Rad, Cat. #4561096). Proteins were transferred onto precut low-fluorescence polyvinylidene diflu-

oride membranes (Bio-Rad, Cat. #1620261) and blocked with 5% non-fat dry milk in Tris-buffered saline with 0.1% Tween 20 (TBST) for 1 h at room temperature. Membranes were then incubated overnight at 4°C with primary antibodies diluted in TBST containing 5% non-fat dry milk. After washing the membranes with TBST (three 5-min washes), they were incubated with HRP-linked secondary antibodies diluted in TBST with 5% non-fat dry milk for 1 h at room temperature. Following another series of washes with TBST (three 5-min washes), the blots were developed using Clarity Western ECL substrate (Bio-Rad, Cat. #1705061) and imaged with a ChemiDoc imaging system (Bio-Rad).

RNA isolation and RT-qPCR assay

Total RNAs were isolated from control or treated cells using TRIzol reagent (Invitrogen, Cat. #15596-018), following the manufacturer's protocol. For RT-qPCR assays, total RNA was pretreated with TURBO DNase (Ambion) to remove genomic DNA contamination, before reverse transcription into cDNA using iScript Reverse Transcription Supermix (Bio-Rad, Cat. #1708840). An aliquot of 20–50 ng of cDNA and a Forward/Reverse primer set (Sigma) were used in each PCR reaction. Real-time PCR was performed in triplicate or quadruplicate using SsoAdvanced Universal SYBR Green Supermix (Bio-Rad, Cat. #1725270). The primers used for qPCR are listed in Supplementary Table S1. Level of mRNA expression for each gene was normalized by expression of the reference gene 18S rRNA and calculated using the 2[−Delta Delta C(T))] method [38].

CRISPR/Cas9 gene editing

DNMT3B-deficient NCI-H1299 cell lines were generated by CRISPR/Cas9 gene editing, as described previously [39]. In brief, each gBlock (Integrated DNA Technologies) containing the sequence of a U6 promoter-driven, single guide RNA (sgRNA) and the *pCAG-Cas9-IRES-GFP* plasmid were co-transfected in NCI-H1299 cells using Lipofectamine 2000 (Invitrogen). At 24 h post-transfection, GFP-positive cells were sorted and then seeded, at low density, in six-well culture plates to derive individual clones. Two sgRNAs were used to target *DNMT3B*, one targeting exon 6 and the other, exon 18 (Supplementary Fig. S2C and Supplementary Table S1). *DNMT3B*-mutant clones were identified by DNA sequencing and verified by immunoblotting.

Colony formation assay

A549 cells and various genotypes of NCI-H1299 cells (parental and untargeted controls and two *DNMT3B* KO clones) were seeded in 12-well culture plates at a density of 2000 cells per well. The following day, cells were treated with 0.1% DMSO or GSK-3484862 at concentrations ranging from 0.1 to 2.0 μM (A549) or 0.4 μM (NCI-H1299). Culture medium was replaced with fresh medium containing either DMSO or compound every other day. After 8 days (NCI-H1299) or 10 days (A549) of treatment, cells were washed twice with tap water and then stained with 0.5% crystal violet solution at room temperature for 20 min with gentle shaking on a bench rocker. Crystal violet power was purchased from Fisher Scientific (Cat. #C581-25) and dissolved in 20% methanol. After staining, cells were washed with water and air-dried before image scanning.

Cell viability assay

Four cell lines, NCI-H1299 parental cells, untargeted control cells, and two *DNMT3B* KO cell lines were seeded in 96-well culture plates at a density of ∼500 cells per well. The following day, cells were treated with 0.1% DMSO or 0.4 μM GSK-3484862. Culture medium along with either DMSO or fresh compound was replenished every other day. On day 8, cells were collected and viability was assessed using the CellTiter-Glo Luminescent Cell Viability Assay Kit (Promega, Cat. #G7572), following the manufacturer's instructions.

Genomic DNA isolation

NCI-H1299 parental, untargeted control, and two *DNMT3B* KO cell lines were seeded in 60-mm culture dishes. The next day, cells were treated with 0.1% DMSO or 2 μM GSK-3484862. The culture medium with DMSO or compound was replenished every other day. At days 2 and 6, cells were harvested and their genomic DNA was extracted using a Quick-DNA Miniprep Kit (Zymo Research, Cat. #D3025), following the manufacturer's instructions.

Bisulfite pyrosequencing methylation analysis

We applied bisulfite PCR amplification followed by pyrosequencing methylation analyses to evaluate the DNA methylation changes in cell lines treated with DMSO or GSK-3484862 with varied concentrations and times. PCR primers for pyrosequencing methylation analysis shown in Supplementary Table S1 were used in the analyses of selected CpG sites in the promoter region of *DNMT3B*, *CDX1*, *NKX2-6*, *RASSF1A*, and *TERT* (telomerase reverse transcriptase), and within the DNA sequences of D4Z4, NBL2, αSat, and LINE-1. The assays for D4Z4, NBL2, αSat, and LINE-1 were first described by Choi *et al.* [40]. All procedures have been previously described [32]. In brief, an aliquot of bisulfite-converted DNA (40 ng) was used for each PCR amplification and the amplification products were sequenced using a PyroMark Q96 ID instrument (Qiagen). Each reaction included controls for high methylation (M.SssI-treated DNA), low methylation via whole genome amplification (WGA)-amplified DNA, and no-DNA template. DNA methylation values of biological and technical replicates were averaged to report DNA methylation levels per sample, per assay. All steps were performed by the Epigenomics Profiling Core at the University of Texas MD Anderson Cancer Center.

Mass spectrometry analysis

DNA samples were digested to nucleosides using Nucleoside Digestion Mix (New England Biolabs, Cat. #M0649S). Liquid chromatography tandem mass spectrometry (LC-MS/MS) analysis was performed by injecting digested DNAs on an Agilent 1290 Infinity II UHPLC equipped with a G7117A diode array detector and a 6495C triple quadrupole mass detector operating in the positive electrospray ionization mode (+ESI). UHPLC was carried out on a Waters XSelect HSS T3 XP column (2.1 mm × 100 mm, 2.5 μm) with a gradient mobile phase consisting of methanol and 10 mM aqueous ammonium acetate (pH 4.5). MS data acquisition was performed in the dynamic multiple reaction monitoring (DMRM) mode. Each nucleoside was identified in the extracted chromatogram associated with its specific MS/MS transition: dC $[M + H]^+$ at m/z 228.1→112.1, 5mdC $[M + H]^+$ at m/z 242.1→126.1,

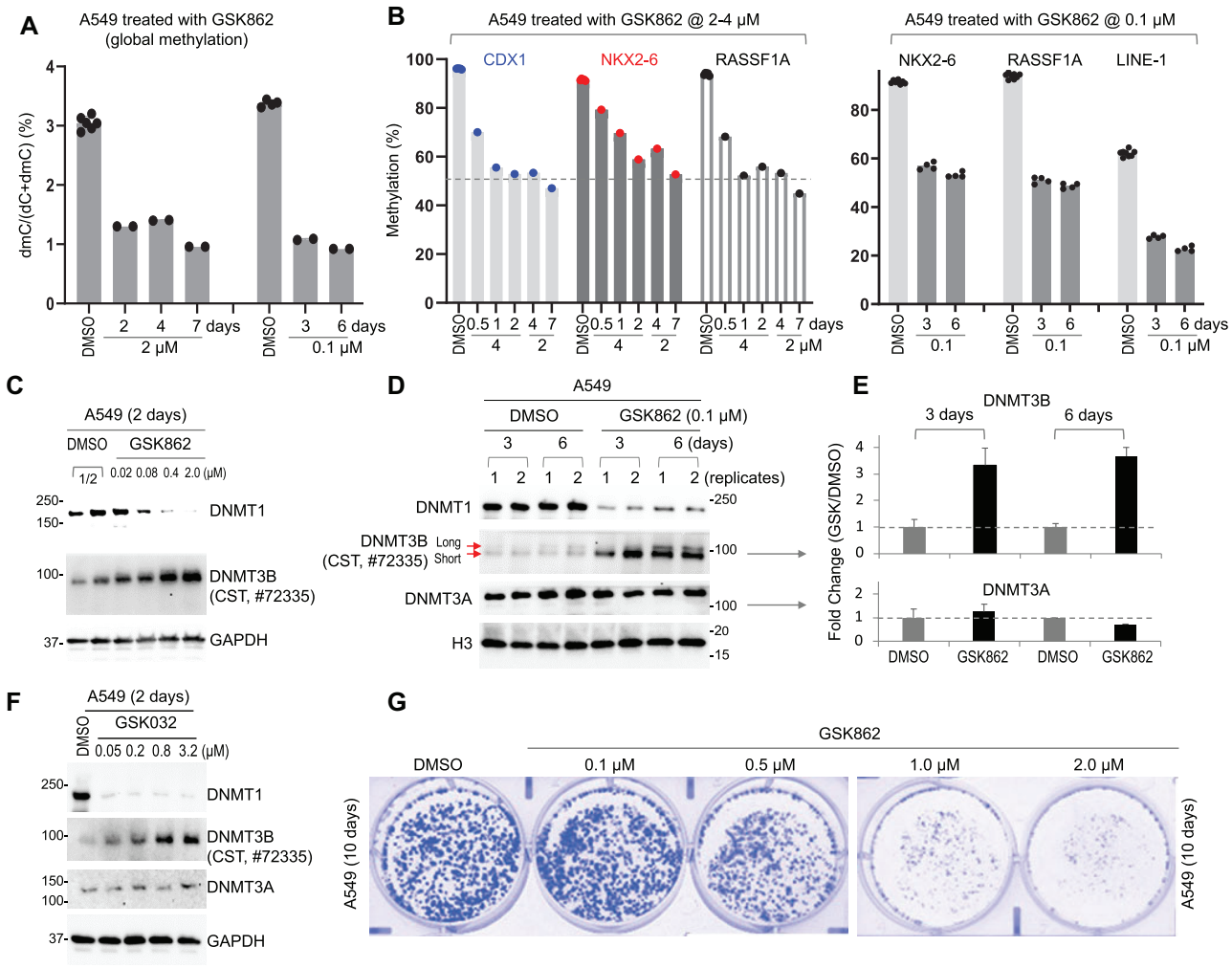

Figure 1. GSK-3484862 (labeled as GSK862) depletes DNMT1 protein and increases DNMT3B protein. (**A**) Mass spectrometry analysis of total 5mC content in A549 cells expressed as a percentage (i.e. number of 5mC-modified residues divided by the total number of cytosine residues × 100). The DMSO controls at different time points were averaged. (**B**) GSK862 induced hypomethylation, as determined by pyrosequencing, at three genomic loci (*CDX1*, *NKX2-6,* and *RASSF1A*) and at multiple transposable *LINE-1* elements in A549 cells, as a function of treatment time and variation of compound concentrations. (**C**) Western blots showing endogenous levels of DNMT1 and DNMT3B in A549 cells following a 2-day treatment with GSK862 concentrations ranging from 0.02 to 2.0 μM. Note that the sample amount in the first lane was half of that in the other lanes. (**D**) Western blots showing increases of DNMT3B isoforms (indicated by arrows for long and short) and no changes in DNMT3A after treatment with GSK862. (**E**) Plots of intensities of protein bands of DNMT3A and DNMT3B shown in panel (D). (**F**) Concentration-dependent effect of GSK-3685032 (labeled as GSK032) in A549 cells. (**G**) Colony formation assay of A549 cells treated at the indicated doses of GSK862 for 10 days.

and dT $[M + H]^+$ at m/z 243.1→127.1. External calibration curves prepared using known amounts of the nucleosides were used to calculate nucleoside ratios in the analyzed samples.

Results

Lung cancer cells treated with DNMT1 degrader GSK-3484862 had increased DNMT3B protein levels

Previously, we demonstrated that dicyanopydridine-containing GSK compounds feature a planar dicyanopyridine moiety that competes with DNMT1's active-site loop for intercalation into the DNMT1-bound DNA, specifically between the two base pairs of CpG dinucleotides [28, 29]. In cells, this trapping of DNMT1 on chromatin-associated DNA promotes its degradation, leading to DNA demethylation [32]. However, treating A549 lung cancer cells with GSK-3484862 decreased both global and locus-specific DNA methylation, an effect that plateaued after 2 days of treatment (Fig. 1A and B). In pyrosequencing assays, demethylation was detectable as early as 12 h after treatment but there were minimal subsequent changes after 24–48 h of treatment. Unexpectedly, GSK-3484862 had a concentration-dependent effect (Fig. 1C) that both increased DNMT3B (but not DNMT3A) protein levels and decreased DNMT1 levels (Fig. 1C–E). Previous studies have shown that multiple *DNMT3B* isoforms exist in lung cancer cell lines due to alternative promoter usage and/or splicing (see Supplementary Fig. S2A and B) [41, 42]. Western blot analysis performed with an antibody (CST, #72335) that recognizes a region common to most (if not all) known DNMT3B isoforms revealed that DNMT3B isoform levels increased after treatment with GSK-3484862 (Fig. 1D). This increase in DNMT3B protein level was also observed following GSK-3484862 treatment of the lung cancer cell line NCI-H1299 (Fig. 2A), as well as with

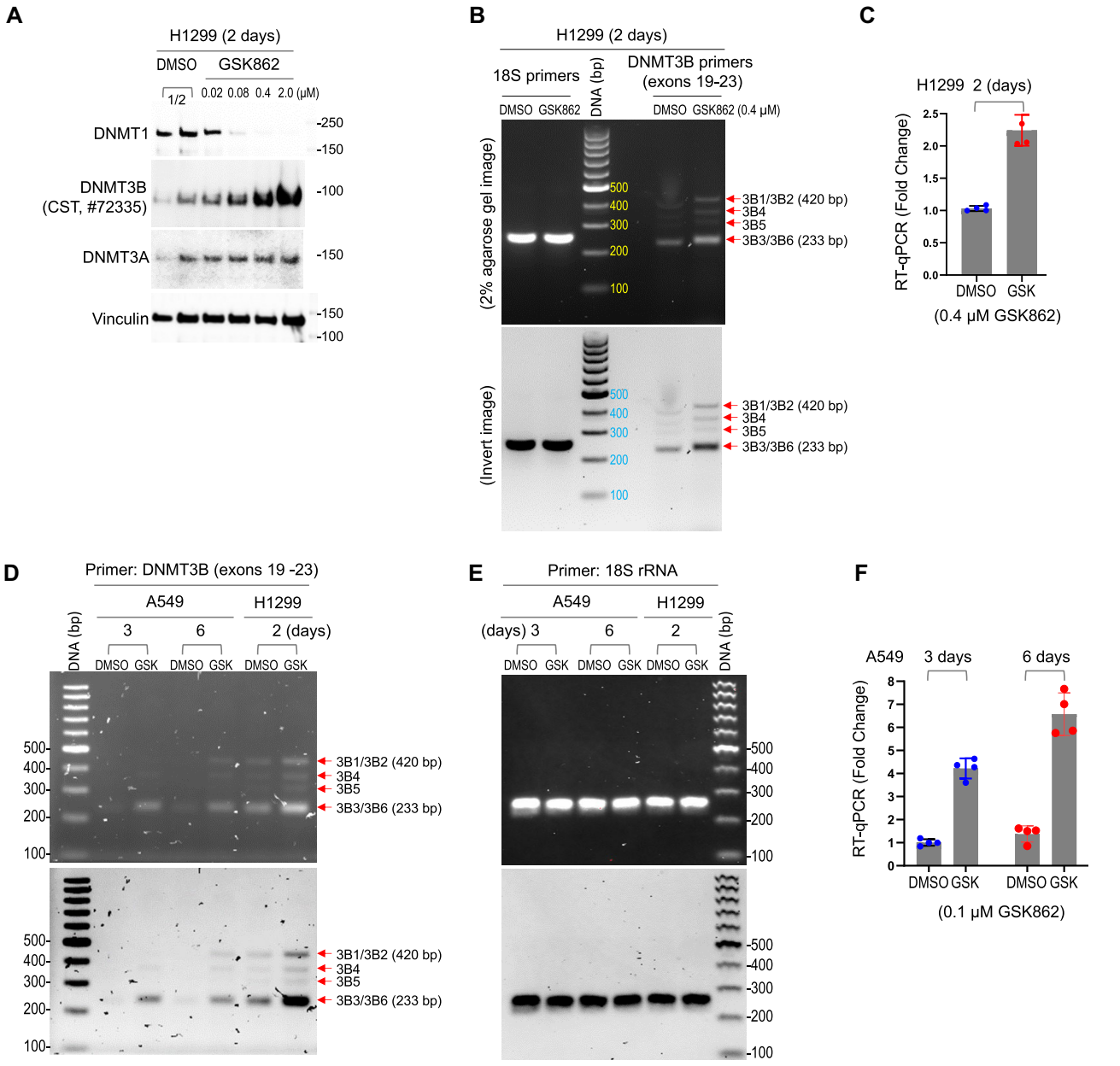

Figure 2. GSK-3484862 (labeled as GSK862 or GSK) upregulates *DNMT3B* transcripts in A549 and NCI-H1299 cells. (**A**) Concentration-dependent effect of GSK862 in NCI-H1299 cells after 2 days of treatment at the indicated concentrations. Note that the sample amount in the first lane was half of that in the other lanes. (**B**) RT-PCR analysis (at 28 cycles) of *DNMT3B* expression in NCI-H1299 cells after 2 days of GSK862 (0.4 μM) or mock (DMSO) treatment. The expression of 18S rRNA was used as a control. The qPCR products or amplicons were analyzed in a 2% agarose gel. (**C**) Relative expression of *DNMT3B* in NCI-H1299 cells was analyzed by RT-qPCR (at 39 cycles) after 2 days of GSK862 (0.4 μM) or mock (DMSO) treatment. (**D**) Expression of *DNMT3B* and (**E**) 18S rRNA in A549 and NCI-H1299 cell lines as assessed by RT-PCR (at 28 cycles) after the indicated number of days of GSK862 (0.1 μM) or mock (DMSO) treatment. The qPCR products or amplicons were analyzed in 2% agarose gels. (**F**) Relative expression of *DNMT3B* in A439 cells was analyzed by RT-qPCR (at 39 cycles) following GSK-862 (0.1 μM) or mock (DMSO) treatment for 3 or 6 days.

the related compound GSK-3685032 in A549 cells (Fig. 1F), showing that the effect was neither cell line nor GSK compound specific. These findings suggest a complex interplay between DNMT1 depletion and DNMT3B upregulation in response to these dicyanopyridine-containing compounds. Nevertheless, extended treatment of A549 cells with GSK-3484862 (over a 10-day period at concentrations up to 2 μM) resulted in progressively enhanced growth inhibition (Fig. 1G) as previously reported for GSK-3484862 treatment of leukemia cells (MV4-11) [28] and colorectal cancer cells (HCT116 and RKO) [36].

GSK-3484862 upregulates *DNMT3B* transcripts

The human *DNMT3B* gene has 23 exons and is located on chromosome 20q11.21 (Supplementary Fig. S2A). *DNMT3B* produces numerous splice variants that include or exclude exons 10, 21, and/or 22 [42] (Supplementary Fig. S2B). To investigate whether the GSK compound-induced increase in DNMT3B protein (Fig. 2A) was due to upregulation at the transcript level, we performed RT-PCR analysis by amplifying a region from exons 19 to 23 within the methyltransferase catalytic domain. This approach can distinguish variants containing exons 21 and 22 (*DNMT3B1/3B2*), lacking both ex-

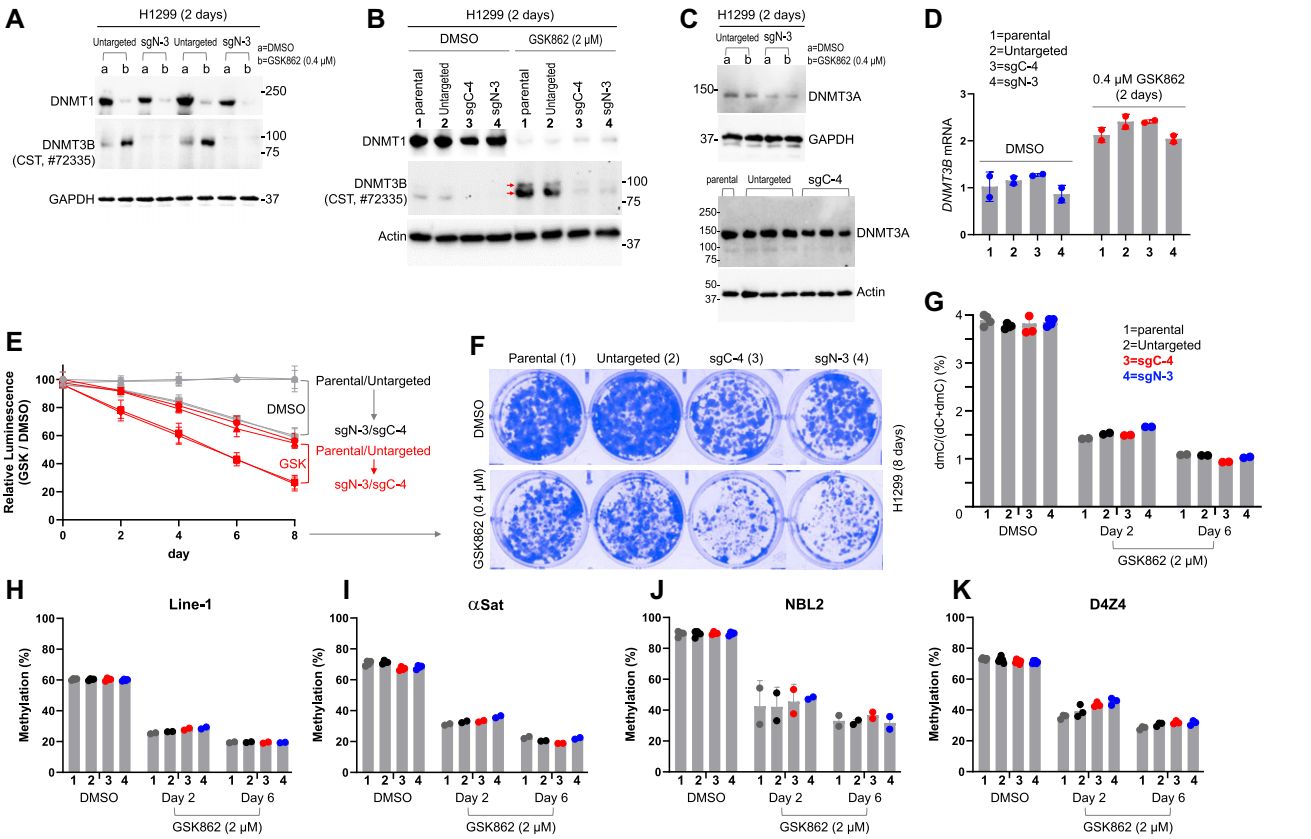

Figure 3. *DNMT3B*-deficient NCI-H1299 cells are more sensitive to the growth-inhibitory effect of GSK-3484862 (labeled as GSK862 or GSK). (**A**) Western blots showing *DNMT3B* KO cell line sgN-3 lack DNMT3B protein expression following 2 days of GSK862 (0.4 μM) or mock (DMSO) treatment ($N = 2$ replicates). (**B**) As in panel (A) but also including the parental and untargeted cell lines and two KO cells lines (sgN-3 and sgC-4) using a much higher concentration (2 μM) of GSK-3484862. (**C**) Western blot showing CRIPSR/Cas9 gene editing has no or minimal effect on DNMT3A protein levels (top panels: sgN-3; bottom panels: sgC-4 with $N = 3$ replicates). (**D**) *DNMT3B* mRNA levels were unaffected in *DNMT3B* KO cells relative to control cells in the absence of GSK-3484862, but all cell lines displayed an approximately two-fold increase in *DNMT3B* mRNA levels following treatment with GSK-3484862 at 0.4 μM for 2 days. (**E**) Cell viability assays showing enhanced sensitivity of *DNMT3B*-deficient NCI-H1299 cells to GSK-3484862. (**F**) Colony formation assay showing that GSK-3484862 treatment significantly inhibited cell growth of *DNMT3B*-deficient NCI-H1299 cells compared to WT (parental and untargeted) NCI-H1299 cells (top panels: DMSO treatment; bottom panels: GSK treatment). (**G**) Mass spectrometry analysis of total 5mC content expressed as a percentage (i.e. number of 5mC-modified residues divided by the total number of cytosine residues × 100). (**H**–**K**) GSK-3484862 induced hypomethylation at four genomic loci (*LINE-1*, *Sat*, *NBL2*, and *DAZ4*) in NCI-H1299 cells, measured by pyrosequencing, following GSK-3484862 treatment at 2 μM for 2 or 6 days.

ons 21 and 22 (*DNMT3B3/3B6*), and missing either exon 21 (*DNMT3B4*) or exon 22 (*DNMT3B5*) (Supplementary Fig. S2B). In both NCI-H1299 cells (Fig. 2B and C) and A549 cells (Fig. 2D–F), treatment with GSK-3484862 increased the expression of each of these transcripts. Notably, both cell lines predominately expressed *DNMT3B* isoforms that lack exons 21 and 22 (e.g. *DNMT3B3/3B6*), consistent with previous observations in lung cancer cell lines [42]. Additionally, *DNMT3B* overexpression is common in cancer patients from TCGA datasets [43], and *DNMT3B3* is a predominant isoform expressed in various human cancers, as revealed by analysis of TCGA data [44]. Notably, catalytically inactive DNMT3B isoforms, such as DNMT3B3, can form tetrameric complexes with active DNMT3 isoforms (DNMT3A1, 3A2, 3B1, and 3B2) and enhance their enzymatic activity [45].

DNMT3B deficiency sensitizes NCI-H1299 cells to GSK-3484862-induced growth and viability inhibition

DNMT3B upregulation could be a compensatory response to DNMT1 depletion and inhibition, which may make the GSK compounds less efficacious. To explore the possibility, we disrupted the *DNMT3B* gene in NCI-H1299 cells with CRISPR/Cas9 gene editing using two sgRNAs: one targeting exon 6 in the N-terminal unstructured region (sgN), and one targeting exon 18 in the catalytic domain (sgC). We recovered clones with frameshift indels on both alleles from both sgRNAs (Supplementary Fig. S2C). We confirmed that these *DNMT3B* KO clones (sgN-3 and sgC-4) lacked DNMT3B protein expression (Fig. 3A and B), while having no or minimal effect on DNTM3A protein levels (Fig. 3C). Notably, these deletions did not alter *DNMT3B* mRNA levels, but treatment of cells with GSK-3484862 at 0.4 μM for 2 days increased *DNMT3B* mRNA levels by approximately two-fold (Fig. 3D). Although treatment of wild-type (WT, i.e. parental and untargeted) NCI-H1299 cells with GSK-3484862 resulted in a modest inhibition of cell viability and growth, *DNMT3B*-deficient NCI-H1299 cells were substantially more sensitive to the compound (Fig. 3E and F). These findings suggest that DNMT3B plays a role in modulating cellular responses to GSK-3484862 and that a combination of DNMT1 and DNMT3B inhibitors or pan-DNMT inhibitors would likely have stronger cell growth-inhibitory effects.

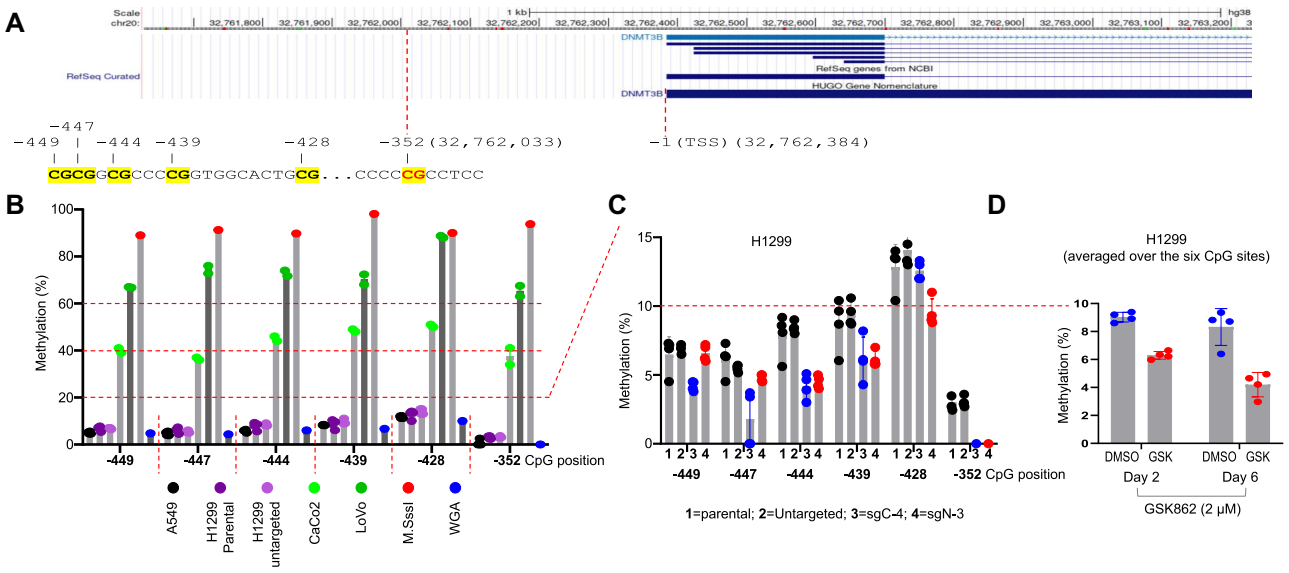

Figure 4. *DNMT3B* promoter hypomethylation in A549 and NCI-H1299 cells. (**A**) Schematic representation of the six CpG sites located upstream of the TSS of *DNMT3B*. (**B**) Quantitative measurement of CpG methylation by pyrosequencing in two lung cancer cell lines (A549 and NCI-H1299) and two colon cancer cell lines (CaCo2 and LoVo). In NCI-H1299 cells, the residual methylation levels (10%–15%) at the upstream CpG sites were further reduced by CRIPSR edits (sgN-3 and sgC-4) (**C**) or treatment with GSK-3484862 (**D**).

We next quantified the 5-methylcytosine (5mC) content on fully digested genomic DNA from DMSO- or GSK-3484862-treated NCI-H1299 cells, including WT (parental and untargeted) controls and two *DNMT3B* KO cell lines, using mass spectrometry. *DNMT3B* deficiency did not affect 5mC level in NCI-H1299 cells. Both DMSO-treated control and *DNMT3B* KO cells had ~3.8% of their cytosines methylated (Fig. 3G). Following GSK-3484862 treatment, 5mC levels showed similar decreases in all cell lines, dropping to ~1.5% at day 2 and ~1.0% at day 6 (Fig. 3G). Given the overt effect of *DNMT3B* deficiency on GSK-3484862-induced inhibition of cell viability and growth (Fig. 3E and F), the observation that 5mC levels showed only small differences between the *DNMT3B* KO and control cell lines was somewhat unexpected. Unlike mESCs, which can survive and proliferate without DNA methylation [46–48], human cancer cell lines and human embryonic stem cells cannot tolerate a severe loss of global DNA methylation [49, 50]. As a result, cells exhibiting only mild hypomethylation may gain a growth advantage in culture, potentially obscuring the overall impact of *DNMT3B* deficiency on global 5mC levels. Alternatively, the increased sensitivity of *DNMT3B* KO cells to GSK-3484862 may stem from hypomethylation of specific genes—such as tumor suppressor genes—whose expression becomes detrimental to cellular survival.

Using the same samples analyzed by mass spectrometry, we performed pyrosequencing at four repetitive elements loci: interspersed repeats (*LINE1*) and tandem repeats (*αSat*, *NBL2*, and *D4Z4*) (Fig. 3H–K). These sites were chosen because DNA hypomethylation of repetitive elements is a common feature in cancer [40] and were previously reported to be hypomethylated in DNMT3B-asscoaited ICF (immunodeficiency, centromeric instability, and facial abnormalities) syndrome [51–53]. We found that demethylation at individual loci following GSK-3484862 treatment mirrored the global demethylation pattern we observed.

GSK-induced *DNMT3B* upregulation in NCI-H1299 is associated with hypomethylation of *DNMT3B* regulatory elements

To gain insights into the mechanisms by which the DNMT1 inhibitor/degrader induces *DNMT3B* upregulation, we measured the methylation levels of various CpG sites in the *DNMT3B* locus. A previous study of methylation in human colorectal cancer cell lines reported that the CpG site located 352 bp upstream of the transcription start site (TSS) of *DNMT3B* (Fig. 4A) is completely unmethylated in non-tumorigenic colon tissues but is hypermethylated to varying degrees in most colorectal cancer cells [54]. Therefore, we initially investigated methylation at this site (−352 bp), plus five additional upstream sites, in A549 and NCI-H1299 cells. We found that the two lung cancer cell lines showed no or low DNA methylation (<10%) at these CpG sites (Fig. 4B). In addition, no DNA methylation is present immediately near the *DNMT3B* TSS in A549 cells, according to information available in the UCSC Genome Browser summarizing reduced representation bisulfite sequencing (RRBS) and Illumina's Infinium HumanMethylation 450 BeadChip data from ENCODE.

However, the corresponding CpG sites in CaCo2 cells (a human epithelial cell derived from a colon carcinoma) and LoVo cells (a human colon cancer cell line) were methylated at ~40% and 60%–70%, respectively (Fig. 4B). Controls for high methylation (M.SssI-treated DNA) and low methylation (WGA-amplified DNA) were included to confirm the accuracy of our DNA methylation analyses and exclude technical reasons for the observed opposing methylation levels between lung (low methylation) and colon cancer (high methylation) cells (Fig. 4B). The results indicate cell/cancer type-specific methylation patterns around the −352-bp region. In NCI-H1299 cells, the residual methylation levels at these CpG sites were further decreased by *DNMT3B* disruption (sgN-3 and sgC-4) (Fig. 4C) or GSK-3484862 treatment (Fig. 4D).

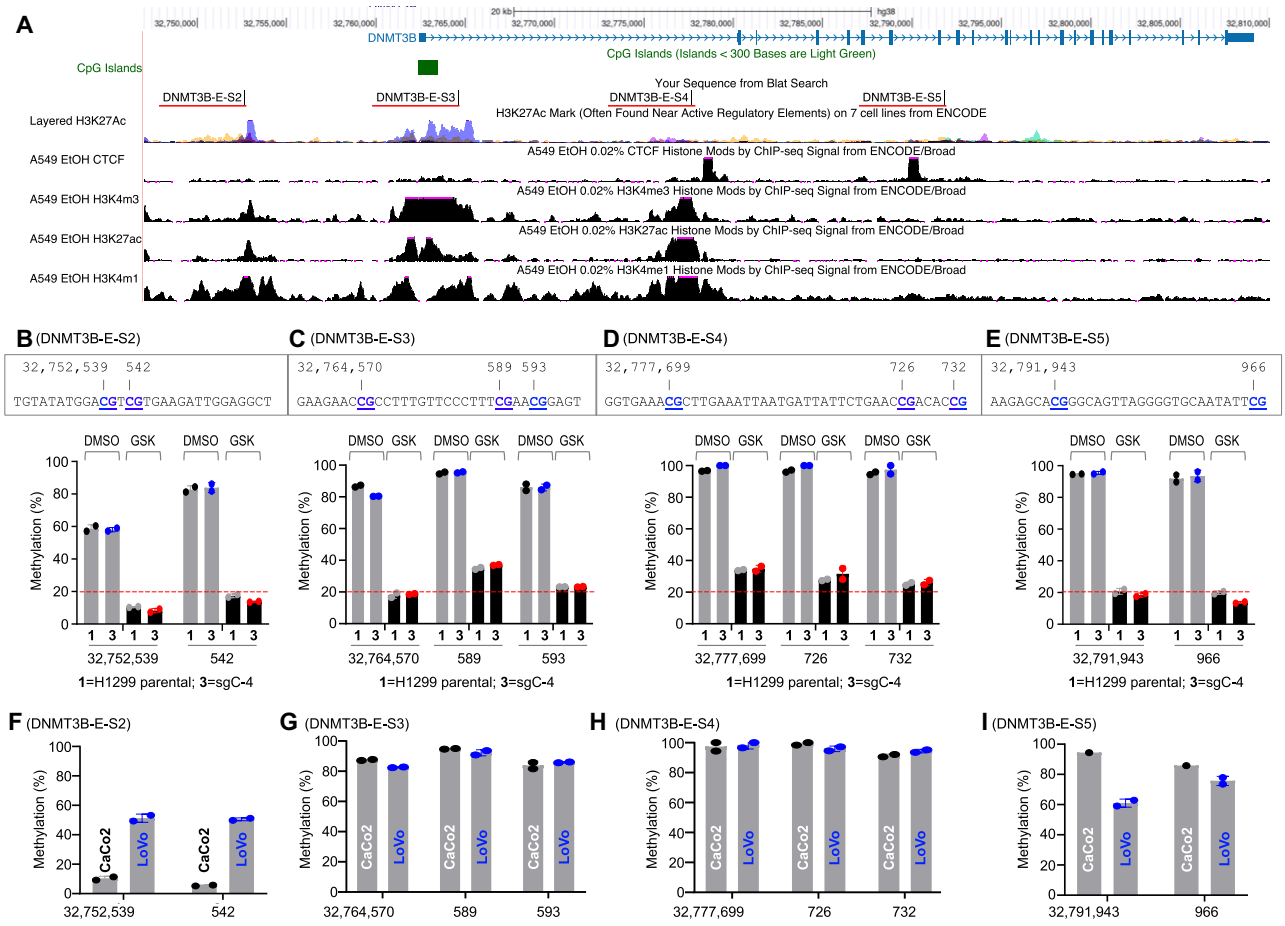

Figure 5. Analysis of CpG methylation in potential *DNMT3B* regulatory elements in NCI-H1299 cells. (**A**) Selections of four regions, S2, S3, S4, and S5, associated with the *DNMT3B* gene on chr 20 based on histone marks and CTCF binding (all data publicly available on UCSC Genome Browser as visual representation of ENCODE ChIP-seq experiments). (**B**–**E**) Quantitative measurement of CpG methylation by pyrosequencing in parental and *DNMT3B* KO (sgC-4) NCI-H1299 cells, with GSK-3484862 treatment or without (DMSO). (**F**–**I**) Quantitative measurement of CpG methylation by pyrosequencing in two colon cancer cell lines (CaCo2 and LoVo).

We next examined four additional regions of the *DNMT3B* gene—the S2 region (−10 kb; located 10 kb upstream of the TSS), the S3 region (+2 kb; 2kb downstream of the TSS), the S4 region (+15 kb), and the S5 region (+30 kb)—that are potential regulatory elements based on the ENCODE ChIP-seq enrichment of enhancer/promoter histone marks (H3K27ac, H3K4me1/me3) and/or proximity to CTCF-binding sites in A549 cells [55] (Fig. 5A). At the S2 region, two CpG positions showed respectively methylation levels of ∼60% and ∼80% in parental and *DNMT3B* KO (sgC-4) NCI-H1299 cells (Fig. 5B). Treatment with the GSK compound significantly reduced methylation at these positions to below 20% (Fig. 5B). Similarly, CpG positions within the S3, S4, and S5 regions were highly methylated (over 80%, with some approaching 100%). GSK compound treatment reduced the methylation levels at these sites to 20%–30% (Fig. 5C–E). Compared to the average genome-wide demethylation level of ∼50%, the GSK compound appears to exert a more pronounced demethylating effects on these hypermethylated CpG dinucleotides associated with the *DNMT3B* gene.

As a control, we analyzed methylation levels at these CpG sites in CaCo2 and LoVo, two colon cancer cell lines with differing *DNMT3B* expression. CaCo2 exhibits high *DNMT3B* expression, with a $\log_2$(TPM+1) value of 5.87, placing it among the top 25 cell lines out of nearly 1,700 in the 24Q4 batch-corrected gene expression dataset available on DepMap (https://depmap.org/portal/). In contrast, LoVo shows low DNMT3B expression at $\log_2$(TPM+1) of 1.86, ranking below position 1,000. Our pyrosequencing methylation analysis showed that in CaCo2 cells, the DNA methylation at the two CpG sites within the S2 region was low (<10%), whereas LoVo cells displayed ∼50% methylation at the same sites (Fig. 5F). In contrast, both cell lines showed similar levels of hypermethylation in the S3 and S4 regions, and between 60% and 90% methylation in the S5 region (Fig. 5G–I).

In summary, GSK compound-induced DNMT1 depletion and inhibition results in a severe loss of DNA methylation across multiple *DNMT3B*-associated regions that are normally hypermethylated in NCI-H1299. Hypomethylation at these regulatory elements may contribute to *DNMT3B* upregulation. Given the inverse relationship between CpG methylation at the S2 region and *DNMT3B* expression in the colon cancer cell lines CaCo2 and LoVo, we tentatively speculate that the S2 region, located ∼10 kb upstream of the TSS of *DNMT3B*, is part of an enhancer involved in regulating *DNMT3B* expression.

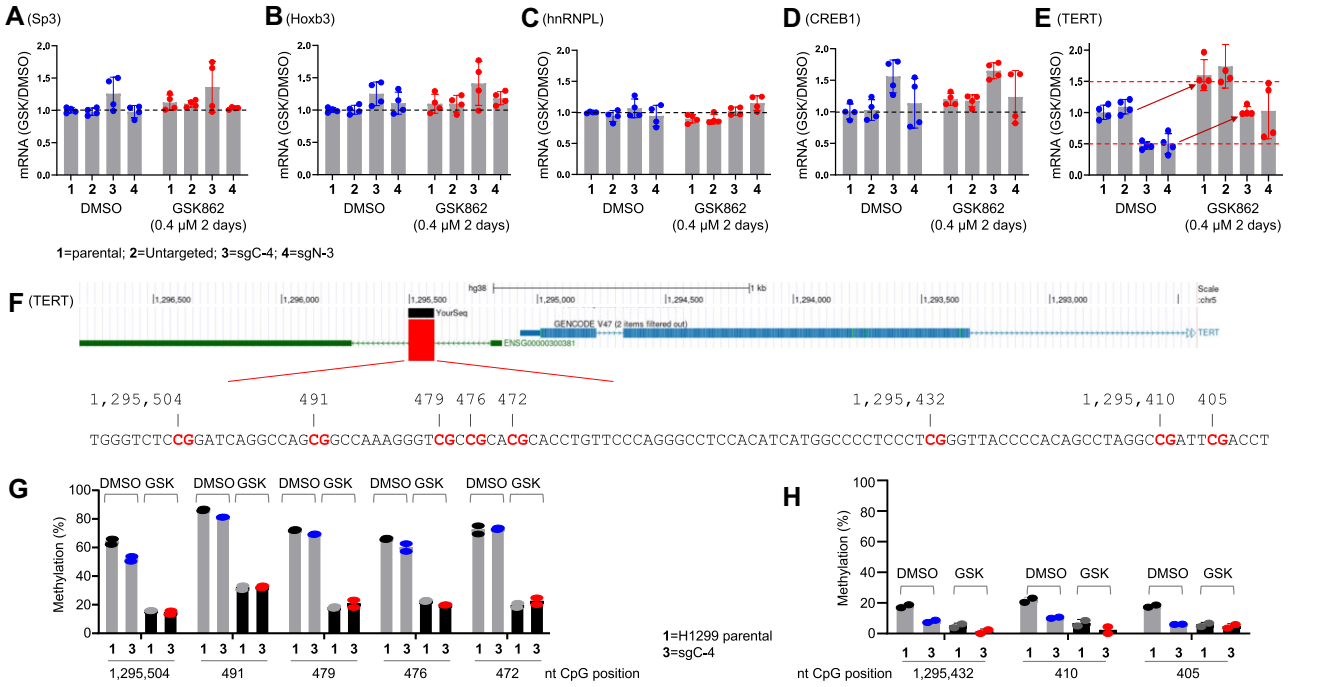

Figure 6. Candidate transcription factors involved in *DNMT3B* expression. (**A**–**E**) RT-PCR analysis of *SP3, HOXB3, HNRNPL, CREB1,* and *TERT* expression following GSK-3484862 treatment (0.4 μM for 2 days) in NCI-H1299 cells. (**F**) Schematic representation of the promoter CpG sites located upstream of the TSS of *TERT,* highlighted by a block. (**G**, **H**) Quantitative measurement by pyrosequencing in NCI-H1299 of (**G**) five CpG hypermethylation sites and (**H**) three CpG hypomethylation sites.

Candidate transcription factors involved in *DNMT3B* expression

We also investigated the expression of several genes previously shown to regulate *DNMT3B* expression. In HEK293 cells, the transcription factor SP3 increases *DNMT3B* mRNA expression four-fold [56]. Likewise, *HOXB3* and *DNMT3B* are overexpressed in a correlated manner in human lung adenocarcinoma samples [57]. In hepatocellular carcinoma, TERT is required for aberrant *DNMT3B* expression [58], and in HeLa cells, the transcription factor CREB binds to the *DNMT3B* promoter and induces its transcription [59]. Additionally, a study in male mouse embryonic stem cells showed that hnRNPL (heterogeneous nuclear ribonucleoprotein L), a splicing factor that promotes exon inclusion, interacts with RNA polymerase II at the *Dnmt3b* promoter to facilitate a switch from the inactive *Dnmt3b6* isoform to the active *Dnmt3b1* isoform [60].

In NCI-H1299 cells, we found that the mRNA expression levels of *SP3*, *HOXB3*, and the *HNRNPL* gene (which encodes the splicing factor hnRNPL) showed little or no change after treatment with GSK-3484862 (Fig. 6A–C). For the *CREB1* gene, the two *DNMT3B* KO cell lines displayed different responses: sgC-4 showed an increased *CREB1* expression, while sgN-3 showed no change (Fig. 6D). However, treatment with GSK-3484862 had no effect on *CREB1* expression. In contrast, *TERT* expression was decreased by 50% in both *DNMT3B* KO cell lines (Fig. 6E), consistent with previous findings showing reduced *TERT* expression upon *DNMT3B* silencing in A172 and SW1088 human glioma cell lines [61] and in HCT116 colorectal carcinoma cells [62] (Supplementary Fig. S3). Notably, *TERT* expression in both parental and *DNMT3B* KO NCI-H1299 cells increased ~1.5–2× following GSK-3484862 treatment (Fig. 6E).

A recent study revealed that *TERT* activation promotes DNMT3B-mediated hypermethylation in primary human cells [63]. Additionally, *TERT* expression is known to be regulated by DNA methylation of its promoter region [58, 61, 64, 65]. We further analyzed a previously characterized set of five hypermethylated CpG sites located ~400 bp upstream of the TSS of *TERT* promoter [65] (Fig. 6F). In the parental and the sgC-4 KO NCI-H1299 cells, these five CpG sites were methylated at levels of 60%–90%, which decreased to 20%–30% following GSK-3484862 treatment (Fig. 6G). In contrast, three CpG sites located ~40 and ~60 nucleotides away exhibited low methylation levels (10%–20%) (Fig. 6H). These findings indicate that CpG site-specific methylation can vary substantially within a relatively short genomic region of ~100 base pairs.

Discussion

Altered DNA methylation is a universal feature of human tumors, highlighting the critical role of methylation in cancer initiation, progression, and adaption (reviewed in [66]). Tumor-associated DNA methylation changes involve two contrasting processes: locus-specific hypermethylation, which contributes to the inactivation of tumor suppressor and other regulatory genes, and global hypomethylation, which is associated with chromosomal instability, reactivation of transposable elements, loss of genomic imprinting, and eventual tumor heterogeneity [67]. These opposing processes may interact and cooperate in tumorigenesis, representing a "yin-and-yang" dynamic. This duality complicates pharmacological intervention, as it is challenging to reverse these opposite effects to achieve a balanced, homeostatic state using a single small-molecule compound. Nevertheless, demethylat-

ing agents, such as azacytidine and decitabine, have proven to benefit patients with hematologic malignancies. The discovery of dicyanopyridine-containing DNMT1-selective inhibitors by GSK [28] has raised the prospect of developing specific and potent DNMT inhibitors as therapeutics that may overcome some major drawbacks of nucleoside analogs, including their toxicity and ineffectiveness in treating solid tumors.

Here, we demonstrate that inhibition and depletion of DNMT1 by compound GSK-3484862 result in upregulation of *DNMT3B* expression in two lung cancer cell lines, A549 and NCI-H1299. *DNMT3B* upregulation is likely a compensatory response to aid cancer cell survival and progression. In support of this notion, genetic ablation of *DNMT3B* substantially sensitizes NCI-H1299 cells to GSK-3484862-induced inhibition of cell viability and growth. Although the catalytically inactive DNMT3B3 and/or 3B6 isoforms appear to be the major isoforms expressed in A549 and NCI-H1299 cells and are upregulated in response to GSK compounds, they can form tetrameric complexes with active DNMT3A and 3B isoforms, stimulating their *de novo* enzymatic activity [45, 60, 68–70]. This DNMT3L-like accessory function of DNMT3B3/3B6 may help maintain the low DNA methylation level required for tumor cell survival [71–73]. Our findings suggest that a combination treatment targeting both DNMT1 and DNMT3A/B or using pan-DNMT inhibitors could exert stronger growth-inhibitory effects on tumor cells, potentially preventing the development of resistance [36]. We note that a recent study using an inducible DNMT1 degradation in a pseudo-diploid colorectal carcinoma epithelial cell line (DLD-1) for 4 days also observed an upregulation of DNMT3B with no changes in overall DNMT3A levels [74]. Together with our findings, this suggested a complementary and cooperative relationship between DNMT1 and DNMT3B in maintaining and regulating overall genomic DNA methylation.

Previous work has implicated hypermethylation of a *DNMT3B* promoter region (around the −352 bp CpG site) in the repression of *DNMT3B* expression in human colorectal cancer [54]. However, our pyrosequencing analysis revealed that this promoter region around the −352 bp CpG site is unmethylated in both A549 and NCI-H1299 cells. Instead, we identified a candidate enhancer located approximately ∼10 kb upstream of the *DNMT3B* TSS that is hypermethylated in NCI-H1299 cells. Treatment with GSK-3484862 induces demethylation at this enhancer, which may directly contribute to the upregulation of *DNMT3B* expression. These findings suggest that *DNMT3B* expression is regulated by methylation of regulatory elements in a manner that is specific to the cancer type or cell context.

While *DNMT3B* upregulation can be explained by GSK-3484862-induced loss of methylation at its enhancer/promoter regions, the mechanisms involved could be more complex. For example, we found that a subset of five CpG sites in the *TERT* promoter is hypermethylated in NCI-H1299 cells, consistent with previous observations in pediatric brain tumors [65]. Treatment with GSK-3484862 induces demethylation at the *TERT* promoter and increases *TERT* expression, which may enable TERT protein to bind directly to the *DNMT3B* promoter, as observed in human iPSC derived neurons [63]. This potential TERT-DNMT3B feedback loop has been hypothesized [75]. Further research is needed to clarify the role of TERT—whether as a reverse transcriptase enzyme or as a DNA-binding protein—and to explore the therapeutic potential of TERT inhibitor/degrader [76] targeting the TERT-DNMT3B feedback loop in controlling cell-type-specific, DNMT3B-mediated methylation.

DNA methylation acts in concert with other epigenetic mechanisms to regulate gene expression and other biological processes. A potential alternative approach could involve combining a DNA demethylating agent with inhibitors of histone modifying enzymes. For example, histone deacetylase (HDAC) inhibitors have been evaluated in combination with nucleoside analogs azacytidine or decitabine in preclinical and clinical studies [77–82]. However, the efficacy of this combination has been limited by toxicity [80]. Reassessing this strategy using the newly developed, non-nucleoside DNMT1-selective inhibitor/degrader in combination with next-generation HDAC inhibitors [83, 84] may be warranted. In summary, the interplay between cancer-associated epigenetic abnormalities, such as altered DNA methylation and histone modifications, highlights the potential of therapeutic strategies aimed at reprogramming tumor cells. This approach could involve the use of drugs targeting multiple epigenetic pathways to achieve more effective treatment outcomes.

Acknowledgements

We thank Dr Briana Dennehey for editing the manuscript and insightful comments. We thank the anonymous reviewers for their thoughtful suggestions. MD Anderson Cancer Center's Epigenomics Profiling Core performed pyrosequencing.

Author contributions: Qin Chen [Data curation], Swanand Hardikar [Data curation], Kimie Kondo [Data curation], Nan Dai [Data curation], Ivan R. Corrêa Jr [Supervision], Meigen Yu [Formal analysis], Marcos R. Estecio [Investigation; Supervision], Xing Zhang [Conceptualization; Project administration], Taiping Chen [Funding acquisition; Supervision; Writing - review & editing], Xiaodong Cheng [Conceptualization; Funding acquisition; Supervision; Writing - original draft].

Supplementary data

Supplementary data is available at NAR Cancer online.

Conflict of interest

N.D. and I.R.C. are employees of New England Biolabs, Inc., a manufacturer and vendor of molecular biology reagents. This affiliation does not affect the authors' impartiality, adherence to journal standards and policies, or availability of data. The other authors declare no competing interests.

Funding

The work was supported by the U.S. National Institutes of Health (R35GM134744 to X.C., R21CA277152 to T.C. and X.C.), the Cancer Prevention and Research Institute of Texas (RR160029 to X.C.). M.Y. is supported by a training fellowship from the Gulf Coast Consortia on the National Library of Medicine Training Program in Biomedical Informatics and Data Science (T15LM007093). This research was also partly supported by funds from the Texas Tobacco Settlement–Molecular Mechanisms of Tobacco Carcinogenesis. T.C. and X.C. are CPRIT Scholars in Cancer Research. The MDACC Epigenomics Profiling Core was supported in

part by The University of Texas MD Anderson Cancer Center and the Center for Cancer Epigenetics.

Data availability

The data underlying this article are available in the article and in its online supplementary material.

References

1. Bird AP. DNA methylation versus gene expression. *J Embryol Exp Morphol* 1984;**83**:31–40.
2. van der Ploeg LH, Groffen J, Flavell RA. A novel type of secondary modification of two CCGG residues in the human gamma delta beta-globin gene locus. *Nucleic Acids Res* 1980;**8**:4563–74. https://doi.org/10.1093/nar/8.20.4563
3. van der Ploeg LH, Flavell RA. DNA methylation in the human gamma delta beta-globin locus in erythroid and nonerythroid tissues. *Cell* 1980;**19**:947–58. https://doi.org/10.1016/0092-8674(80)90086-0
4. Shen CK, Maniatis T. Tissue-specific DNA methylation in a cluster of rabbit beta-like globin genes. *Proc Natl Acad Sci USA* 1980;**77**:6634–8. https://doi.org/10.1073/pnas.77.11.6634
5. Greger V, Passarge E, Hopping W *et al.* Epigenetic changes may contribute to the formation and spontaneous regression of retinoblastoma. *Hum Genet* 1989;**83**:155–8. https://doi.org/10.1007/BF00286709
6. Stirzaker C, Millar DS, Paul CL *et al.* Extensive DNA methylation spanning the Rb promoter in retinoblastoma tumors. *Cancer Res* 1997;**57**:2229–37.
7. Sakai T, Toguchida J, Ohtani N *et al.* Allele-specific hypermethylation of the retinoblastoma tumor-suppressor gene. *Am J Hum Genet* 1991;**48**:880–8.
8. Herman JG, Latif F, Weng Y *et al.* Silencing of the VHL tumor-suppressor gene by DNA methylation in renal carcinoma. *Proc Natl Acad Sci USA* 1994;**91**:9700–4. https://doi.org/10.1073/pnas.91.21.9700
9. Kuroki T, Trapasso F, Yendamuri S *et al.* Allele loss and promoter hypermethylation of VHL, RAR-beta, RASSF1A, and FHIT tumor suppressor genes on chromosome 3p in esophageal squamous cell carcinoma. *Cancer Res* 2003;**63**:3724–8.
10. Merlo A, Herman JG, Mao L *et al.* 5' CpG island methylation is associated with transcriptional silencing of the tumour suppressor p16/CDKN2/MTS1 in human cancers. *Nat Med* 1995;**1**:686–92. https://doi.org/10.1038/nm0795-686
11. Herman JG, Merlo A, Mao L *et al.* Inactivation of the CDKN2/p16/MTS1 gene is frequently associated with aberrant DNA methylation in all common human cancers. *Cancer Res* 1995;**55**:4525–30.
12. Gonzalez-Zulueta M, Bender CM, Yang AS *et al.* Methylation of the 5' CpG island of the p16/CDKN2 tumor suppressor gene in normal and transformed human tissues correlates with gene silencing. *Cancer Res* 1995;**55**:4531–5.
13. Yoon JH, Dammann R, Pfeifer GP. Hypermethylation of the CpG island of the RASSF1A gene in ovarian and renal cell carcinomas. *Int J Cancer* 2001;**94**:212–7. https://doi.org/10.1002/ijc.1466
14. Dammann R, Yang G, Pfeifer GP. Hypermethylation of the cpG island of Ras association domain family 1A (RASSF1A), a putative tumor suppressor gene from the 3p21.3 locus, occurs in a large percentage of human breast cancers. *Cancer Res* 2001;**61**:3105–9.
15. Agathanggelou A, Honorio S, Macartney DP *et al.* Methylation associated inactivation of RASSF1A from region 3p21.3 in lung, breast and ovarian tumours. *Oncogene* 2001;**20**:1509–18. https://doi.org/10.1038/sj.onc.1204175
16. Astuti D, Agathanggelou A, Honorio S *et al.* RASSF1A promoter region CpG island hypermethylation in phaeochromocytomas and neuroblastoma tumours. *Oncogene* 2001;**20**:7573–7. https://doi.org/10.1038/sj.onc.1204968
17. Santi DV, Norment A, Garrett CE. Covalent bond formation between a DNA-cytosine methyltransferase and DNA containing 5-azacytosine. *Proc Natl Acad Sci USA* 1984;**81**:6993–7. https://doi.org/10.1073/pnas.81.22.6993
18. Sheikhnejad G, Brank A, Christman JK *et al.* Mechanism of inhibition of DNA (cytosine C5)-methyltransferases by oligodeoxyribonucleotides containing 5,6-dihydro-5-azacytosine. *J Mol Biol* 1999;**285**:2021–34. https://doi.org/10.1006/jmbi.1998.2426
19. Ganesan A, Arimondo PB, Rots MG *et al.* The timeline of epigenetic drug discovery: from reality to dreams. *Clin Epigenetics* 2019;**11**:174. https://doi.org/10.1186/s13148-019-0776-0
20. Lopez M, Gilbert J, Contreras J *et al.* Inhibitors of DNA Methylation. *Adv Exp Med Biol* 2022;**1389**:471–513.
21. Neuendorff NR, Gagelmann N, Singhal S *et al.* Hypomethylating agent-based therapies in older adults with acute myeloid leukemia - a joint review by the Young International Society of Geriatric Oncology and European Society for Blood and Marrow Transplantation Trainee Committee. *J Geriatr Oncol* 2023;**14**:101406. https://doi.org/10.1016/j.jgo.2022.11.005
22. Juttermann R, Li E, Jaenisch R. Toxicity of 5-aza-2′-deoxycytidine to mammalian cells is mediated primarily by covalent trapping of DNA methyltransferase rather than DNA demethylation. *Proc Natl Acad Sci USA* 1994;**91**:11797–801. https://doi.org/10.1073/pnas.91.25.11797
23. Sato T, Issa JJ, Kropf P. DNA hypomethylating drugs in cancer therapy. *Cold Spring Harb Perspect Med* 2017;**7**:a026948. https://doi.org/10.1101/cshperspect.a026948
24. Bewersdorf JP, Zeidan AM. Management of higher risk myelodysplastic syndromes after hypomethylating agents failure: are we about to exit the black hole? *Expert Rev Hematol* 2020;**13**:1131–42. https://doi.org/10.1080/17474086.2020.1819233
25. Stomper J, Rotondo JC, Greve G *et al.* Hypomethylating agents (HMA) for the treatment of acute myeloid leukemia and myelodysplastic syndromes: mechanisms of resistance and novel HMA-based therapies. *Leukemia* 2021;**35**:1873–89. https://doi.org/10.1038/s41375-021-01218-0
26. Wong KK. DNMT1: A key drug target in triple-negative breast cancer. *Semin Cancer Biol* 2021;**72**:198–213. https://doi.org/10.1016/j.semcancer.2020.05.010
27. Wong KK. DNMT1 as a therapeutic target in pancreatic cancer: mechanisms and clinical implications. *Cell Oncol (Dordr)* 2020;**43**:779–92. https://doi.org/10.1007/s13402-020-00526-4
28. Pappalardi MB, Keenan K, Cockerill M *et al.* Discovery of a first-in-class reversible DNMT1-selective inhibitor with improved tolerability and efficacy in acute myeloid leukemia. *Nat Cancer* 2021;**2**:1002–17. https://doi.org/10.1038/s43018-021-00249-x
29. Horton JR, Pathuri S, Wong K *et al.* Structural characterization of dicyanopyridine containing DNMT1-selective, non-nucleoside inhibitors. *Structure* 2022;**30**:793–802.https://doi.org/10.1016/j.str.2022.03.009
30. Gilmartin AG, Groy A, Gore ER *et al. In vitro* and *in vivo* induction of fetal hemoglobin with a reversible and selective DNMT1 inhibitor. *Haematologica* 2021;**106**:1979–87. https://doi.org/10.3324/haematol.2020.248658
31. Azevedo Portilho N, Saini D, Hossain I *et al.* The DNMT1 inhibitor GSK-3484862 mediates global demethylation in murine embryonic stem cells. *Epigenetics Chromatin* 2021;**14**:56.
32. Chen Q, Liu B, Zeng Y *et al.* GSK-3484862 targets DNMT1 for degradation in cells. *NAR Cancer* 2023;**5**:zcad022. https://doi.org/10.1093/narcan/zcad022
33. Ge F, Wang Y, Chen P *et al.* FOXN3-AS1: a candidate prognostic marker and epigenetic target with immunotherapeutic implications in acute myeloid leukemia. *Curr Med Chem* 2024; https://doi.org/10.2174/0109298673311108240926062214.
34. Xiao H, Li X, Liang S *et al.* Dual-responsive nanomedicine activates programmed antitumor immunity through targeting lymphatic system. *ACS Nano* 2024;**18**:11070–83. https://doi.org/10.1021/acsnano.3c11464

35. Eldeeb D, Okada H, Suzuki Y *et al.* Exploring the role of DNMT1 in dental papilla cell fate specification during mouse tooth germ development through integrated single-cell transcriptomics and bulk RNA sequencing. *J Oral Biosci* 2024;**66**:530–8. https://doi.org/10.1016/j.job.2024.06.010
36. Wiseman AK, Tiedemann RL, Fan H *et al.* Chromosome-specific retention of cancer-associated DNA hypermethylation following pharmacological inhibition of DNMT1. *Commun Biol* 2022;**5**:528. https://doi.org/10.1038/s42003-022-03509-3
37. Chen T, Ueda Y, Xie S *et al.* A novel Dnmt3a isoform produced from an alternative promoter localizes to euchromatin and its expression correlates with active *de novo* methylation. *J Biol Chem* 2002;**277**:38746–54. https://doi.org/10.1074/jbc.M205312200
38. Livak KJ, Schmittgen TD. Analysis of relative gene expression data using real-time quantitative PCR and the 2(−Delta Delta C(T)) Method. *Methods* 2001;**25**:402–8. https://doi.org/10.1006/meth.2001.1262
39. Hardikar S, Ying Z, Zeng Y *et al.* The ZBTB24–CDCA7 axis regulates HELLS enrichment at centromeric satellite repeats to facilitate DNA methylation. *Protein Cell* 2020;**11**:214–8. https://doi.org/10.1007/s13238-019-00682-w
40. Choi SH, Worswick S, Byun HM *et al.* Changes in DNA methylation of tandem DNA repeats are different from interspersed repeats in cancer. *Int J Cancer* 2009;**125**:723–9. https://doi.org/10.1002/ijc.24384
41. Wang L, Wang J, Sun S *et al.* A novel DNMT3B subfamily, DeltaDNMT3B, is the predominant form of DNMT3B in non-small cell lung cancer. *Int J Oncol* 2006;**29**:201–7.
42. Ma MZ, Lin R, Carrillo J *et al.* ΔDNMT3B4-del contributes to aberrant DNA methylation patterns in lung tumorigenesis. *EBioMedicine* 2015;**2**:1340–50. https://doi.org/10.1016/j.ebiom.2015.09.002
43. Loaeza-Loaeza J, Cerecedo-Castillo AJ, Rodriguez-Ruiz HA *et al.* DNMT3B overexpression downregulates genes with CpG islands, common motifs, and transcription factor binding sites that interact with DNMT3B. *Sci Rep* 2022;**12**:20839. https://doi.org/10.1038/s41598-022-24186-6
44. Xu TH, Liu M, Zhou XE *et al.* Structure of nucleosome-bound DNA methyltransferases DNMT3A and DNMT3B. *Nature* 2020;**586**:151–5. https://doi.org/10.1038/s41586-020-2747-1
45. Zeng Y, Ren R, Kaur G *et al.* The inactive Dnmt3b3 isoform preferentially enhances Dnmt3b-mediated DNA methylation. *Genes Dev* 2020;**34**:1546–58. https://doi.org/10.1101/gad.341925.120
46. Li E, Bestor TH, Jaenisch R. Targeted mutation of the DNA methyltransferase gene results in embryonic lethality. *Cell* 1992;**69**:915–26. https://doi.org/10.1016/0092-8674(92)90611-F
47. Lei H, Oh SP, Okano M *et al. De novo* DNA cytosine methyltransferase activities in mouse embryonic stem cells. *Development* 1996;**122**:3195–205. https://doi.org/10.1242/dev.122.10.3195
48. Tsumura A, Hayakawa T, Kumaki Y *et al.* Maintenance of self-renewal ability of mouse embryonic stem cells in the absence of DNA methyltransferases Dnmt1, Dnmt3a and Dnmt3b. *Genes Cells* 2006;**11**:805–14. https://doi.org/10.1111/j.1365-2443.2006.00984.x
49. Chen T, Hevi S, Gay F *et al.* Complete inactivation of DNMT1 leads to mitotic catastrophe in human cancer cells. *Nat Genet* 2007;**39**:391–6. https://doi.org/10.1038/ng1982
50. Liao J, Karnik R, Gu H *et al.* Targeted disruption of DNMT1, DNMT3A and DNMT3B in human embryonic stem cells. *Nat Genet* 2015;**47**:469–78. https://doi.org/10.1038/ng.3258
51. Miniou P, Jeanpierre M, Bourc'his D *et al.* Alpha-satellite DNA methylation in normal individuals and in ICF patients: heterogeneous methylation of constitutive heterochromatin in adult and fetal tissues. *Hum Genet* 1997;**99**:738–45. https://doi.org/10.1007/s004390050441
52. Kondo T, Bobek MP, Kuick R *et al.* Whole-genome methylation scan in ICF syndrome: hypomethylation of non-satellite DNA repeats D4Z4 and NBL2. *Hum Mol Genet* 2000;**9**:597–604. https://doi.org/10.1093/hmg/9.4.597
53. Hansen RS. X inactivation-specific methylation of LINE-1 elements by DNMT3B: implications for the Lyon repeat hypothesis. *Hum Mol Genet* 2003;**12**:2559–67. https://doi.org/10.1093/hmg/ddg268
54. Huidobro C, Urdinguio RG, Rodriguez RM *et al.* A DNA methylation signature associated with aberrant promoter DNA hypermethylation of DNMT3B in human colorectal cancer. *Eur J Cancer* 2012;**48**:2270–81. https://doi.org/10.1016/j.ejca.2011.12.019
55. Ram O, Goren A, Amit I *et al.* Combinatorial patterning of chromatin regulators uncovered by genome-wide location analysis in human cells. *Cell* 2011;**147**:1628–39. https://doi.org/10.1016/j.cell.2011.09.057
56. Jinawath A, Miyake S, Yanagisawa Y *et al.* Transcriptional regulation of the human DNA methyltransferase 3A and 3B genes by Sp3 and Sp1 zinc finger proteins. *Biochem J* 2005;**385**:557–64. https://doi.org/10.1042/BJ20040684
57. Palakurthy RK, Wajapeyee N, Santra MK *et al.* Epigenetic silencing of the RASSF1A tumor suppressor gene through HOXB3-mediated induction of DNMT3B expression. *Mol Cell* 2009;**36**:219–30. https://doi.org/10.1016/j.molcel.2009.10.009
58. Yu J, Yuan X, Sjoholm L *et al.* Telomerase reverse transcriptase regulates DNMT3B expression/aberrant DNA methylation phenotype and AKT activation in hepatocellular carcinoma. *Cancer Lett* 2018;**434**:33–41. https://doi.org/10.1016/j.canlet.2018.07.013
59. Ashok C, Selvam M, Ponne S *et al.* CREB acts as a common transcription factor for major epigenetic repressors; DNMT3B, EZH2, CUL4B and E2F6. *Med Oncol* 2020;**37**:68. https://doi.org/10.1007/s12032-020-01395-5
60. Dar MS, Mensah IK, He M *et al.* Dnmt3bas coordinates transcriptional induction and alternative exon inclusion to promote catalytically active Dnmt3b expression. *Cell Rep* 2023;**42**:112587. https://doi.org/10.1016/j.celrep.2023.112587
61. Serifoglu N, Erbaba B, Adams MM *et al.* TERT distal promoter GC islands are critical for telomerase and together with DNMT3B silencing may serve as a senescence-inducing agent in gliomas. *J Neurogenet* 2022;**36**:89–97. https://doi.org/10.1080/01677063.2022.2106371
62. Du Q, Smith GC, Luu PL *et al.* DNA methylation is required to maintain both DNA replication timing precision and 3D genome organization integrity. *Cell Rep* 2021;**36**:109722. https://doi.org/10.1016/j.celrep.2021.109722
63. Shim HS, Iaconelli J, Shang X *et al.* TERT activation targets DNA methylation and multiple aging hallmarks. *Cell* 2024;**187**:4030–42.e13. https://doi.org/10.1016/j.cell.2024.05.048
64. Dogan F, Forsyth NR. TERT promoter methylation is oxygen-sensitive and regulates telomerase activity. *Biomolecules* 2024;**14**:131. https://doi.org/10.3390/biom14010131
65. Castelo-Branco P, Choufani S, Mack S *et al.* Methylation of the TERT promoter and risk stratification of childhood brain tumours: an integrative genomic and molecular study. *Lancet Oncol* 2013;**14**:534–42. https://doi.org/10.1016/S1470-2045(13)70110-4
66. Esteller M, Dawson MA, Kadoch C *et al.* The epigenetic hallmarks of cancer. *Cancer Discov* 2024;**14**:1783–809. https://doi.org/10.1158/2159-8290.CD-24-0296
67. Besselink N, Keijer J, Vermeulen C *et al.* The genome-wide mutational consequences of DNA hypomethylation. *Sci Rep* 2023;**13**:6874. https://doi.org/10.1038/s41598-023-33932-3
68. Weisenberger DJ, Velicescu M, Cheng JC *et al.* Role of the DNA methyltransferase variant DNMT3b3 in DNA methylation. *Mol Cancer Res* 2004;**2**:62–72. https://doi.org/10.1158/1541-7786.62.2.1
69. Gopalakrishnan S, Van Emburgh BO, Shan J *et al.* A novel DNMT3B splice variant expressed in tumor and pluripotent cells

modulates genomic DNA methylation patterns and displays altered DNA binding. *Mol Cancer Res* 2009;**7**:1622–34. https://doi.org/10.1158/1541-7786.MCR-09-0018
70. Duymich CE, Charlet J, Yang X *et al.* DNMT3B isoforms without catalytic activity stimulate gene body methylation as accessory proteins in somatic cells. *Nat Commun* 2016;**7**:11453. https://doi.org/10.1038/ncomms11453
71. Lapeyre JN, Becker FF. 5-Methylcytosine content of nuclear DNA during chemical hepatocarcinogenesis and in carcinomas which result. *Biochem Biophys Res Commun* 1979;**87**:698–705. https://doi.org/10.1016/0006-291X(79)92015-1
72. Gama-Sosa MA, Slagel VA, Trewyn RW *et al.* The 5-methylcytosine content of DNA from human tumors. *Nucleic Acids Res* 1983;**11**:6883–94. https://doi.org/10.1093/nar/11.19.6883
73. Feinberg AP, Vogelstein B. Hypomethylation distinguishes genes of some human cancers from their normal counterparts. *Nature* 1983;**301**:89–92. https://doi.org/10.1038/301089a0
74. Scelfo A, Barra V, Abdennur N *et al.* Tunable DNMT1 degradation reveals DNMT1/DNMT3B synergy in DNA methylation and genome organization. *J Cell Biol* 2024;**223**:e202307026. https://doi.org/10.1083/jcb.202307026
75. Yuan X, Xu D. Telomerase reverse transcriptase (TERT) in action: cross-talking with epigenetics. *Int J Mol Sci* 2019;**20**:3338. https://doi.org/10.3390/ijms20133338
76. Eglenen-Polat B, Kowash RR, Huang HC *et al.* A telomere-targeting drug depletes cancer initiating cells and promotes anti-tumor immunity in small cell lung cancer. *Nat Commun* 2024;**15**:672. https://doi.org/10.1038/s41467-024-44861-8
77. Issa JP, Garcia-Manero G, Huang X *et al.* Results of phase 2 randomized study of low-dose decitabine with or without valproic acid in patients with myelodysplastic syndrome and acute myelogenous leukemia. *Cancer* 2015;**121**:556–61. https://doi.org/10.1002/cncr.29085
78. Garcia-Manero G, Montalban-Bravo G, Berdeja JG *et al.* Phase 2, randomized, double-blind study of pracinostat in combination with azacitidine in patients with untreated, higher-risk myelodysplastic syndromes. *Cancer* 2017;**123**:994–1002. https://doi.org/10.1002/cncr.30533
79. Ball B, Zeidan A, Gore SD *et al.* Hypomethylating agent combination strategies in myelodysplastic syndromes: hopes and shortcomings. *Leuk Lymphoma* 2017;**58**:1022–36. https://doi.org/10.1080/10428194.2016.1228927
80. Badar T, Atallah E. Do histone deacytelase inhibitors and azacitidine combination hold potential as an effective treatment for high/very-high risk myelodysplastic syndromes? *Expert Opin Investig Drugs* 2021;**30**:665–73. https://doi.org/10.1080/13543784.2021.1915986
81. Moreno Vanegas Y, Badar T. Clinical utility of azacitidine in the management of acute myeloid leukemia: update on patient selection and reported outcomes. *Cancer Manag Res* 2022;**14**:3527–38. https://doi.org/10.2147/CMAR.S271442
82. Zhao A, Zhou H, Yang J *et al.* Epigenetic regulation in hematopoiesis and its implications in the targeted therapy of hematologic malignancies. *Signal Transduct Target Ther* 2023;**8**:71. https://doi.org/10.1038/s41392-023-01342-6
83. Hosseini MS, Sanaat Z, Akbarzadeh MA *et al.* Histone deacetylase inhibitors for leukemia treatment: current status and future directions. *Eur J Med Res* 2024;**29**:514. https://doi.org/10.1186/s40001-024-02108-8
84. Irimia R, Piccaluga PP. Histone deacetylase inhibitors for peripheral T-cell lymphomas. *Cancers (Basel)* 2024;**16**:3359. https://doi.org/10.3390/cancers16193359

Received: January 22, 2025. **Editorial Decision:** May 13, 2025. **Accepted:** May 15, 2025